EVS30 Symposium
Stuttgart, Germany, October 9 - 11, 2017

Battery Testing Methods Assessed from a Policy-Making Perspective: Battery Materials and Cell Performance Testing

A. Pfrang, F. Di Persio, A. Kriston, N. Lebedeva, V. Ruiz, D. Dams, T. Kosmidou, J. Ungeheuer, I. Adanouj, L. Boon-Brett

European Commission, Joint Research Centre (JRC), Directorate for Energy, Transport & Climate, Energy Storage Unit, NL-1755 ZG Petten, The Netherlands

Abstract

Growing international interest in electric vehicles has triggered the need for global harmonization of testing and of type approval of these vehicles and their rechargeable electrical energy storage systems. Multiple testing methods described in scientific literature and in standards, assess battery performance and safety, but are not necessarily appropriate for policy-making purposes. The European Commission's Joint Research Centre tests batteries to assess battery technologies' safety and performance and evaluates testing methods' suitability for policy purposes. An insight into the in-house battery testing capabilities and experimental testing program is provided.

Keywords:

battery, lithium battery, EV (electric vehicle), policy, safety

1 Introduction

Climate change and the mitigation thereof have been in the focus of public interest, but also in the focus of energy policy [1, 2] in the recent years. Ambitious goals set in the European 2030 climate and energy framework require at least a 40 % domestic reduction in greenhouse gas emissions compared to 1990 until 2030 [3] and even an 80-95 % reduction by 2050 [1]. In this context, but also considering the wish of improving security of energy supply and reducing the high cost of oil and gas import into the European Union – in 2014 the EU imported 53 % of the energy it consumed equivalent to around €1 billion per day [4] – specific goals were also set for the transport sector. Road transport still relies quasi exclusively on fossil fuels with oil accounting for 94 % of energy consumed in the transport sector [5]. By 2050, no more conventionally-fuelled cars shall be used in cities and an overall 60 % cut in transport-related greenhouse gas emissions as compared to 1990 levels shall be achieved [6] .

The drive towards these goals is also supported by European legislation, which is not only relevant for the electrification of road transport, but also for the deployment of alternative fuel-powered vehicles in general. Gradually decreasing maximum fleet emission limits for passenger cars are defined (e.g. 95 g CO_2/km by

2021 [7]). Manufacturers are given additional incentives to sell vehicles with extremely low emissions (below 50 g/km) by giving these vehicles a higher weighting for the calculation of the fleet average emissions [7, 8].

Furthermore, the European directive on the deployment of alternative fuels infrastructure aims at the build-up of alternative refuelling infrastructure across Europe using common standards for design and use, which covers also the definition of a common plug for recharging electric vehicles [9].

Against this policy background, batteries are gaining unprecedented recognition as a key enabling technology to achieve Europe's energy, climate and transport goals [10] as well as providing an opportunity for jobs and growth. This sets the scene for increased demands for globally accepted methods for the evaluation of battery performance and safety as new innovative battery technologies are developed to meet the more stringent requirements from users [11]. These demands were addressed in a letter of intent on Electric Vehicle / Smart Grid Interoperability Centres which was signed between the US Department of Energy and the Joint Research Centre [12]. Consequently, the Joint Research Centre (JRC)'s Directorate for Energy, Transport & Climate established in 2013 the BESTEST (Battery Energy Storage Testing for Safe Electrification of Transport) activity [13]. This activity focuses on battery technology as an enabler of electro-mobility. The JRC also examines interoperability issues between the electric vehicles and the charging infrastructure covering hardware and information exchange protocols [14], smart grid aspects and hydrogen/fuel cell technologies [15].

Within the BESTEST activity, pre-normative research is performed supporting the deployment of batteries for vehicle traction with three main pillars:

- Support to electro-mobility policy and international regulations with a focus on the safety of batteries [16-18] – this includes contributions to the development of a UNECE (United Nations Economic Commission for Europe) global technical regulation on electrical vehicle safety [19];
- Harmonisation of energy storage standards for safety and performance test methods and for interoperability [20];
- Supporting innovation and EU industry's global competitiveness through technology validation and stimulating commercialisation – this involves contact and collaboration with industry representative organisations such as Eurobat (Association of European Automotive and Industrial Battery Manufacturers) and EGVIA (European Green Vehicles Initiative Association) [21].

In line with the growing need for robust and impartial research on rechargeable energy storage systems for normative and regulatory purposes [17, 18, 20, 22] and complementing activities in battery modelling [23, 24], experimental facilities at the JRC have been and are being established as described in the following.

2 Laboratory for battery testing at the Joint Research Centre (JRC)

The battery testing laboratories are located in Petten, The Netherlands, and comprise an electrochemical materials and cell performance testing facility established during 2014. Considering the motivation for the installation of the laboratory, it should be emphasized that the focus does not lie on the development or assessment of safety or performance of a specific battery or cell by a specific supplier, but on assessing safety and performance of battery technologies and fitness for purpose of related testing protocols and standards. For this purpose, dedicated and flexible equipment was installed which allows for application of different testing procedures and variation of testing parameters. Furthermore, the laboratory has been designed to facilitate the evaluation of future battery and supercapacitor technologies and the suitability of existing testing methods for these new devices.

2.1 Battery cyclers and temperature chambers

Battery cyclers and potentiostats are used for characterizing the electrochemical performance of batteries/cells (see e.g. 3.1). Three Series 4000 Maccor cyclers provide the largest part of the ca. 100 channels available for battery testing. Number of channels, voltage and current ranges of the three Maccor cyclers are given in Table 1. The accuracy of current is 0.025 % of full scale and of voltage is 0.02 % of full scale. These cyclers can be connected to three frequency response analyzers (Maccor FRA 0355, two

Solatron Analytical Modulab® XM analyzers) through multiplexers allowing automatic interruption of a cycling test by an automatic frequency scan at any time. Ivium potentiostats (Ivium-n-stat and Vertex 5A/IviumBoost1040) equipped for frequency response analysis are also available in the laboratory.

Table 1: Number of channels, voltage and current ranges of Maccor 4000 cyclers.

Cycler	Channels	Voltage range (V)	Current range (A)
1	32	-2 to 8	0 to 20
2	48	-2 to 8	4 ranges: 0 to $150 \cdot 10^{-6}$, 0 to 0.005, 0 to 0.150 and 0 to 5
3	16	0 to 18	0 to 25

The performance of meaningful cycling experiments requires control of temperature, as temperature has a strong influence on battery performance. For this purpose, twelve temperature-controlled test chambers with a volume of approximately 46 l each (distributed between two BiA MTH temperature cabinets) are available with the following specifications: the temperature range is -40 °C to 85 °C with a temperature rate of 2.0 °C/min for both heating and cooling. The temperature deviation in the centre of the working space is ± 0.5 °C.

In case higher heating or cooling rates, compensation of higher heat release rates caused by the sample under test, larger test space volume or control of humidity are required, two Vötsch VCS3 7060-5 climate chambers with a test volume of ca. 600 l can be used. Their specifications are: temperature range is -55 °C to 155 °C with a temperature rate of 6.0 °C/min for both heating and cooling. The temperature deviation in the centre of the working space is ± 0.5 °C. The temperature homogeneity in the overall working space relative to the set value is ± 2.0 °C or better. Heat compensation capacity ranges from 3 kW at -40 °C to 5 kW at temperatures above -20°C. The temperature range for climatic testing is 10 °C to 95 °C with a humidity range of 10 % to 98 % relative humidity.

2.2 Glovebox systems and cell opening procedure

A two glove box system (coupling via a T shaped ante-chamber) and a third independent glove box from MBraun (2x LABmaster SP and MB 200B) are used for assembling and disassembling battery cells and for harvesting materials for further analysis.

The capabilities include decrimping/disassembling of coin cells, pouch cells and cylindrical cells by utilising a decrimper (MTI Corporation), ceramic scissors and an opening tool built in-house. The opening procedure utilised for cylindrical cells – e.g. for harvesting materials for further Scanning Electron Microscopy (SEM) analysis (3.5.1) – deserves more attention and will be described here in detail:

A series of commercial 18650 cells[1] were discharged to the lower cut-off voltage and disassembled. For this the following steps were carried out: 1) determine the thickness of the wall casing (e.g. by computed tomography (CT) imaging of the cell, see Figure 9), 2) lathe-cutting of the cell (see Figure 1a) and 3) use of an opening tool for separating the two parts of the casing without damaging the interior jelly roll (see Figure 1b).

Based on the CT image of the cell, the wall of the casing was around 0.5169 mm. The lathe cut was programmed to penetrate 0.5 mm. The lathe does not fully cut the width of the casing, but leaves a small fraction of steel. The final rupture is realized in the opening tool by pulling apart the two sides of the casing. Once the jelly roll is removed from its casing, the solvent was allowed to evaporate. The active

[1] A123 APR18650M1, lithium iron phosphate/graphite, capacity 1.1 Ah

materials and separator were subsequently dried in a vacuum oven for 4 days at 60 °C and collected for further analysis.

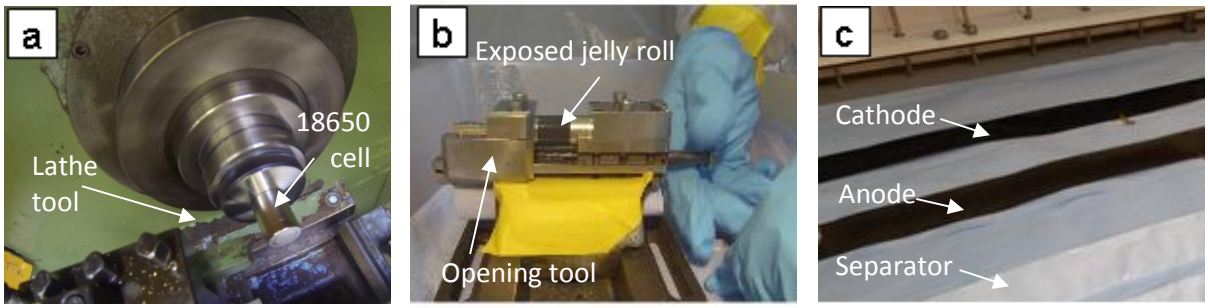

Figure 1: Description of 18650 opening procedure: a) lathe-cutting of the cell, b) opening tool for separating the two parts of the casing and c) cathode, anode and separator material rolls.

2.3 Thermal analysis in combination with gas analysis

An integrated system comprising a Simultaneous Thermal Analysis (STA) instrument connected to a Fourier transform infrared spectrometer (FTIR) and a gas Chromatograph/Mass Spectrometer (GC/MS) is used to gain insight into the thermal degradation of battery components combining gravimetric and calorimetric measurements with subsequent analysis of the evolved gases. A Netzsch STA449F3 Jupiter Simultaneous Thermal Analysis system installed under inert atmosphere in a glove box is connected via heated transfer lines and feedthroughs to a Bruker Vertex 70V FTIR spectrometer and an Agilent 5975C GC/MS, both outside the glove box.

The STA system includes TGA-DSC and TGA-DTA sample carriers and operates either with a silver furnace in the temperature range from -120 °C to 675 °C, using liquid nitrogen for cooling, or with a high-speed furnace in the temperature range from room temperature to 1250 °C. The heating rate with the high speed furnace can be up to 1000 °C/min. The balance of the instrument has a weighing range of up to 35000 mg with resolution of 0.00001 % for thermogravimetric measurements and 1 µW resolution for the differential scanning calorimetry measurements.

The glove box which houses the STA system is equipped with a 0.95 kW cooling unit, for the compensation of the heat generated by the oven and the heated transfer lines.

The Bruker Vertex 70V FTIR spectrometer is equipped with a heated gas cell, installed in the external TGA-IR box, which allows IR measurements of gases coming from the STA to be performed at temperatures up to 200 °C. Heated transfer lines connecting the STA system to the FTIR gas cell are lined with Teflon and can be heated to 200 °C. Infrared spectra can be acquired at a spectral resolution of up to 0.5 cm^{-1} for both configurations.

Additionally, evolved gas is analysed using a gas chromatograph equipped with a mass spectrometer. Gas to be analysed first passes through a fused silica column where corrosive compounds, such as HF, are trapped. Then separation of the evolved gas mixture is performed on HP PLOT U and Molsieve 5A PLOT columns installed in series. The HP PLOT U column consists of bonded, divinylbenzene/ethylene glycol dimethacrylate coated onto a fused silica capillary and is suitable for analysing hydrocarbons (natural gas, refinery gas, C_1-C_7, all C_1-C_3 isomers except propylene and propane); CO_2, CH_4, air, CO, H_2O and polar compounds. Molsieve 5A PLOT column is used for separation of air, Ar, CH_4 and CO.

The Agilent 5975C mass spectrometer offers the possibility to detect a mass range from 5 to 1050 u at a scanning rate of 12.500 u/sec. The Mass Selective Detector operates in the electron ionisation mode, with a high temperature ion source, heatable to 350 °C. The mass filter is a monolithic hyperbolic quadrupole.

Cleaning of the STA furnace, transfer lines and other components after each experiment is commonly performed to avoid cross-contamination of experiments. Thorough cleaning becomes even more important when compounds with boiling points higher than the thermal operational window of the equipment are investigated. As discussed in Section 3.3, the boiling point of ethylene carbonate lies between 247 to

249 °C, while transfer lines, lined with Teflon, as well as other components of the equipment can only be heated up to 200°C. Overnight purging of the entire installation with a (high) air flow while heating all the components to their maximum operating temperature was shown ineffective in this case as evidenced by a weak but still present vibrational signature of ethylene carbonate. Overnight heating under vacuum followed by purging was demonstrated to be sufficient to remove all ethylene carbonate from entire system.

2.4 Thermal imaging

A FLIR A645SC infrared camera equipped with a 25° lens is available for thermal imaging of a cell's surface, but also for thermal imaging of a side-by-side cell (see 2.5). This camera offers an IR resolution of 640×480 pixels at an image frequency of 25 Hz, with a thermal sensitivity better than 0.03 °C at 30 °C. Two ranges of object temperature are available: - 40 °C to 150 °C and 100 °C to 650 °C, with an accuracy of ±2 °C or ±2 % of the reading, whichever is larger.

2.5 In-situ side-by-side IR & optically transparent electrochemical cell

A side-by-side cell (EL-CELL) was equipped with a CaF_2 IR and optically transparent window (see

Figure 2b) aiming at performing in-situ & in-operando evaluation of electrochemical processes (see e.g. 3.2) and also heat release during cycling of battery materials. Both two electrode and three electrode assemblies are possible. Digital imaging can be performed using a Leica MC120HD camera coupled to an Aristomet Leica® microscope (

Figure 2a) or an IR camera (see 2.4) for thermal imaging.

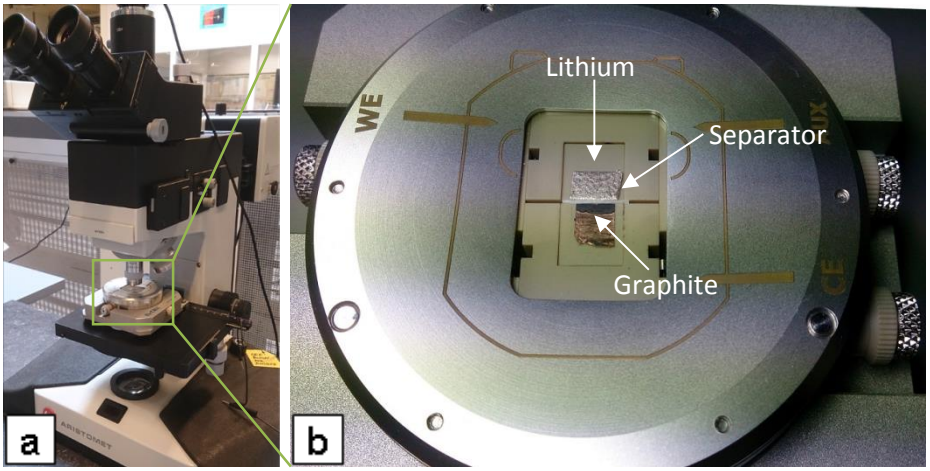

Figure 2: a) Aristomet Leica® optical microscope (coupled to Leica MC120HD camera) and b) transparent side-by-side cell (EL-CELL)

2.6 In-situ dilatometry electrochemical cell

Dilatometry is a powerful tool to evaluate the expansion and contraction of electrode materials upon electrochemical cycling by measuring changes in electrode thickness continuously down to the nanometer range (i.e. <5 nm resolution). In-situ electrochemical dilatometry experiments are performed by utilising an ECD-3-nano dilatometer (EL-CELL®) inside a BIA temperature chamber in combination with a MACCOR Series 4000 cycler (see 3.4). Discs of anode material, 10 mm in diameter, are cycled in a three electrode configuration with a disc of Li foil (Sigma Aldrich) as counter electrode. An additional piece of lithium is used as reference electrode. Charge/discharge cycling was carried out after overnight stabilisation of the cell at 25°C as described in the following: CCCV cycling at 0.2 mA (CV=0.01 mA) in the cut-off voltage range 0.01-1 V vs. Li/Li^+.

2.7 Microstructural analysis

Facilities for microstructural analysis of materials and cell components are also available:

2.7.1 Scanning Electron Microscopy (SEM)

A Zeiss Supra 50VP FEG scanning electron microscope equipped with an Oxford Instruments INCA 350 energy-dispersive X-ray spectroscopy (EDS) system and an Oxford Instruments INCAWave 500 wavelength-dispersive X-ray spectroscopy (WDS) system is used for imaging surfaces (see e.g. 3.5.1) combined with elemental analysis. A Schottky field emitter is used as electron source allowing for spatial resolutions of approx. 1.0 nm at 20 kV and 2.1 nm at 1 kV.

2.7.2 X-ray Computed Tomography (CT)

The Phoenix Nanotom S X-ray CT allows the investigation of samples with a maximum diameter of 120 mm, a maximum height of 200 mm and a maximum weight of 2 kg and is suitable for investigation of cells with a resolution down to ca. 1 µm (see e.g. 3.5.2). This is achieved by using an xs|180nf X-ray tube with a maximum output power of 15 W and a maximum voltage of 180 kV in combination with a 2D detector with a dynamic range of 850:1 which consists of 2300 x 2300 pixels. The X-ray cabinet features two feedthroughs for further connections, e.g. for in-situ imaging. Suitable software – VG Studio MAX (Volume Graphics, Heidelberg, Germany) and MAVI (Fraunhofer ITWM, Kaiserslautern, Germany) – is applied for advanced data analysis [25, 26].

3 Experimental results

The main priorities for the BESTEST activity are the evaluation of performance and safety of battery technologies and assessment of related testing techniques and standards. Examples of experiments performed to this end are presented in the following.

3.1 Battery cycling

One of the key characteristics of a battery cell is its performance over lifetime. Cell degradation is typically investigated by cycling the cell – i.e. repeated charging and discharging – applying a current and voltage profile representative of the intended application (e.g. [27]). From these investigations the lifetime of a cell in this application can be estimated. The definition of lifetime (e.g. end of life at 80 % of initial capacity) also depends on the requirements of the application. In the following, a specific aspect which is the effect of environmental temperature on capacity (e.g. relevant for applications without temperature control), will be discussed.

It is well known that temperature affects the discharge capacity of Li ion batteries and maximum acceptable current during charging [28-30] Temperature also has to be considered when adjusting state of charge (SOC) of a battery which is an important parameter for the battery safety tests [31, 32]. Two different charging-discharging protocols were studied:

1. Charge-discharge at C/3 rate which is equivalent to the conditions defined in IEC standards for BEV applications (the term I_t is used in the standard instead of C-rate, see e.g. IEC 62660-2 [33]), with 20 min relaxation between charge and discharge
2. Constant current 1C – constant voltage (CCCV) charging and constant current 5C discharging (rates as recommended by the manufacturer), with 20 min relaxation between charge and discharge

The tests were executed on 3 A123 APR18650M cells (for details see 2.2) in a temperature chamber (see 2.1). Temperatures representative for laboratory or outdoors environment were selected: between 10 and 40 °C (10, 17, 22, 25, 27 and 40 °C).

The variation in temperature that a cell experiences – which is relevant for cell performance – has two sources: a) environmental temperature variation as set in the temperature chambers and b) the intrinsic thermal variation during charging and discharging. The intrinsic thermal effects of the C/3 protocol are significantly smaller than those of the CCCV protocol due to the higher C-rates used. For both protocols, the self-heating is significant during discharge as compared to negligible or very small self-heating during charge (not shown here).

Figure 3 presents the temperature dependence of normalized discharge capacity. Capacity was normalized by plotting the ratio of capacity vs. capacity measured at 25 °C for each protocol. Analysis of variance (ANOVA) allowed an assessment of the confidence of fit (darker area) and of the confidence of prediction (lighter area).

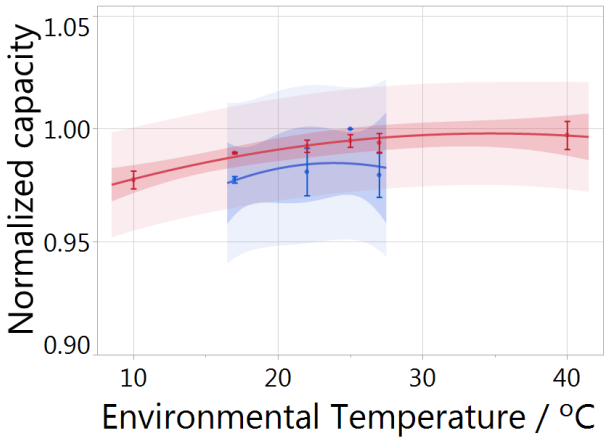

Figure 3: Normalized discharge capacity vs. temperature for A123 APR18650M cells (cycled according to CCCV protocol (red dots) and their fitted model (red line), and cycled according to C/3 protocol (blue dots) and their fitted model (blue line). The darker area is the confidence of fit while the lighter area is the confidence of the prediction. Vertical lines through the dots show the standard deviation of measured values for 4 to 8 repetitions per set of parameters.

The results clearly demonstrate that temperature variations, which can occur from one test setup to another without temperature control (namely within the range of 10 to 40 °C), have a significant impact on discharge capacity. Depending on cell type and applied protocol, the variation of capacity ranges from below 5 % to almost 20 % (supported by data from other cell types not shown here).

3.2 In-situ side-by-side cell investigations of inhomogeneous graphite lithiation

A setup for the in-situ and in-operando evaluation of lithium intercalation during electrochemical cycling for Li ion battery materials has been developed in the BESTEST activity (see 2.5). Some of the preliminary results are described here. A side-by-side graphite-Li cell (EL-CELL®, see

Figure 2) with a CaF_2 transparent window was assembled using 1M $LiPF_6$ solution in EMC:DC:DEC (1:1:1) electrolyte. The experiment consisted in: 1) open circuit voltage (OCV) followed by 2) holding at a potential of 1 mV for 17 hours. Digital imaging was carried out by a MC120HD camera coupled to an Aristomet Leica® microscope. Figure 4 shows a series of optical micrographs of the intercalation of Li into the graphitic structure when holding the cell voltage at 1mV. As indicated by the cell construction previously shown in

Figure 2, the lithium electrode (not shown in the pictures) is placed above the graphite electrode.

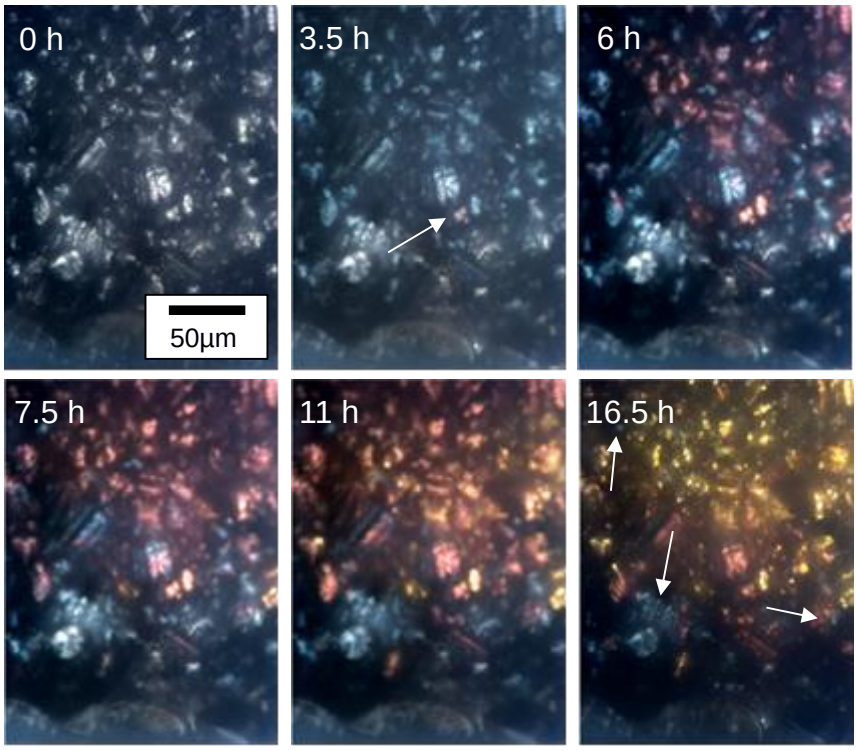

Figure 4: Series of optical micrographs captured at the same location of a graphite electrode over time during a 1mV holding experiment (acquisition time indicated at the top left of each micrograph).

The important features can be summarized as follows: at time 0, where no intercalation has occurred, the picture shows black/grey-coloured graphite particles (Li-free) indicative of A–B–A–B stacking [34]. After 3.5 hours it can be observed that most of the particles turned blue indicating a LiC_{18} structure as new A–A or B–B domains are created. Additionally, it can be observed that some particles are starting to turn red. Over time (t=7.5 h) there is a great proportion of red-coloured particles indicating that the LiC_{12} structure starts to be predominant. However, some particles, particularly those further from the lithium electrode, are still blue. After 11 hours of experiment, gold coloured particles are observed indicating full lithiation. Experimental evidence of the spatial concentration gradient in the intercalation process, can be observed at t=16.5h. Apart from the obvious gradient due to the position of the lithium with respect to the graphite, it can be observed that blue-coloured graphitic particles are surrounded by partially and fully lithiated ones (indicated by the arrows in Figure 4). This implies that the intercalation process is not homogenous. Even after more than 16 hours at a certain voltage, particles show non-uniform lithiation. This could be explained by defects in the graphitic structure, variation in the intra/inter particle electrical contact or in the electrical contact to the current collector, which might initiate local failures (e.g. increased resistance, hot spots) [35, 36]. From this study, it can be concluded that In-situ visible imaging constitutes a promising evaluation tool for the identification of electrode imperfections. The effect that observed lithiation inhomogeneities may have on the long term stability and safety of Li ion batteries will be analysed in future studies.

3.3 Thermal analysis in combination with gas analysis

TGA thermal curve of ethylene carbonate, a solvent which is commonly used in the formulations of contemporary Li ion battery cells, is shown in Figure 5, together with the corresponding Differential Thermal Analysis (DTA) curve and Gram-Schmidt chemigram. At room temperature ethylene carbonate is a solid that usually features large whitish needle-shaped crystals with reported melting point ranging from 35 to 38°C and boiling point from 247 to 249°C, respectively [17]. In good agreement with literature, an endothermic process with an onset temperature of 36°C is observed in the DTA curve (Figure 5). Since it is also not accompanied with any significant weight loss of the sample and because Gram-Schmidt intensity stays constant during the transition, the process can be assigned to melting of ethylene carbonate. As the

sample temperature increases, progressively more ethylene carbonate evaporates leading to a decrease of the sample weight and to an increase of intensity of the endothermic effect. Simultaneously partial pressure of ethylene carbonate increases leading to an increase in the Gram-Schmidt intensity.

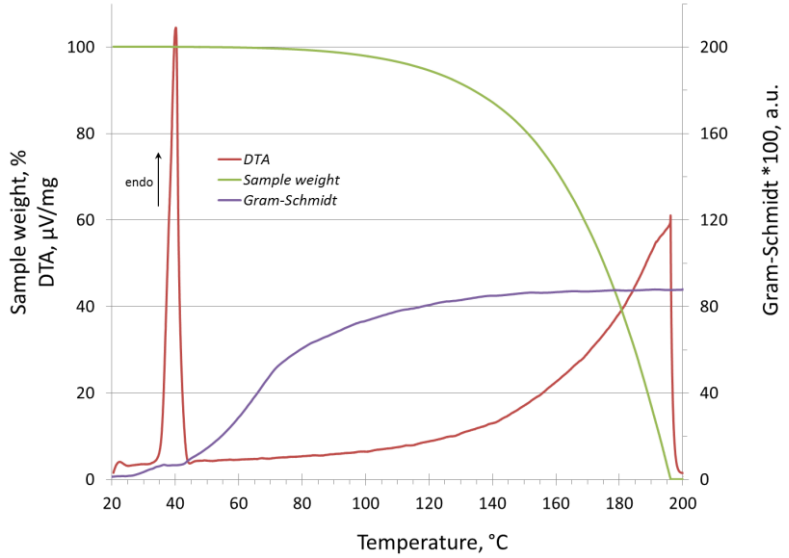

Figure 5: TGA thermal curve of ethylene carbonate with corresponding DTA curve and Gram-Schmidt chemigram. Heating rate 1 K/min, Al_2O_3 crucible, helium flow.

Figure 6 shows an IR spectrum of the gaseous ethylene carbonate recorded during the experiment. In excellent agreement with literature data [37], a number of characteristic peaks are observed. An insert table in Figure 6 lists frequencies of the measured bands with corresponding assignments to the vibrational modes as proposed in [37]. As expected, the most intense band is observed at 1868 cm^{-1}, which corresponds to C=O stretching.

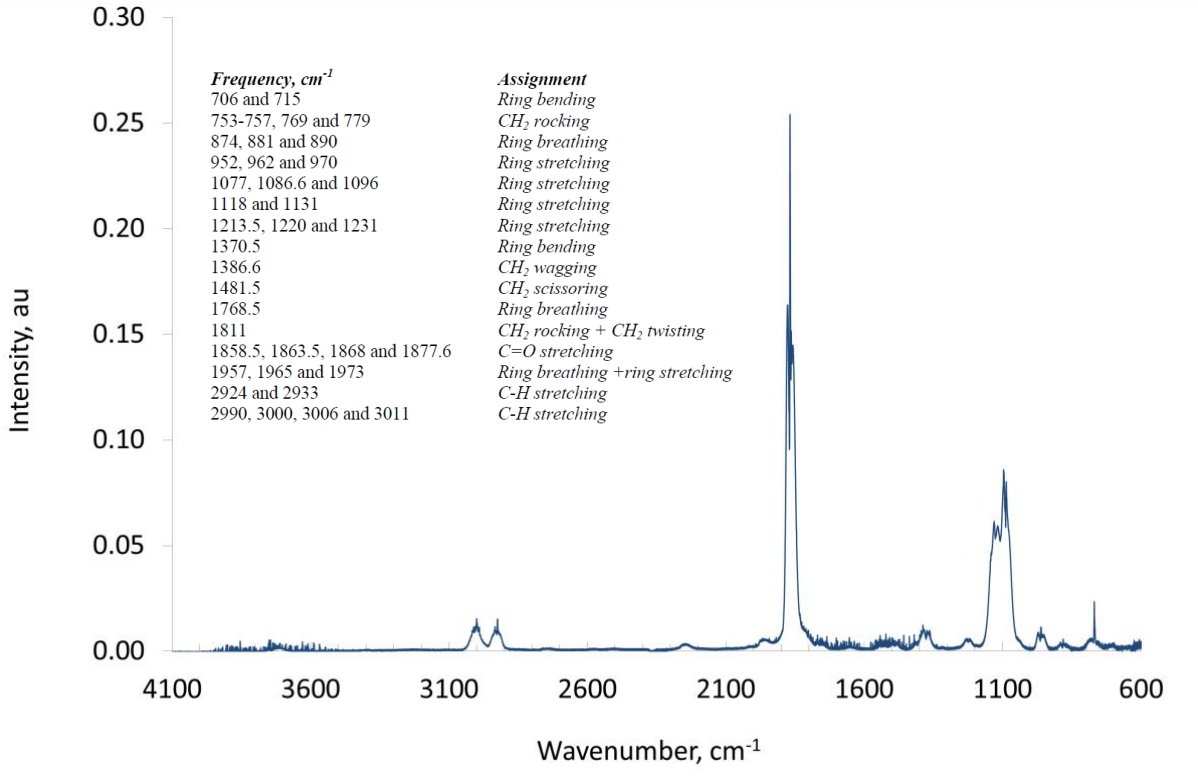

Figure 6: IR spectrum of gaseous ethylene carbonate. Spectrum is recorded at 175°C, spectral resolution 0.5 cm^{-1}.

3.4 Dilatometry investigations of battery electrodes

Figure 7a shows the charge – discharge profile and displacement signal (expansion or contraction of the electrode thickness) of the experiment as described in Section 2.6. As expected, the electrode thickness increases during the intercalation of Li into the graphitic structure and it decreases during the de-intercalation phase. The electrode shows the highest degree of expansion during the first intercalation step, as attributed in the literature to the formation of the SEI layer [38, 39]. During subsequent cycling the expansion and contraction of the electrode shows reversibility. A closer look to the intercalation steps (Figure 7b), allows the identification of the four stages of intercalation, typically described for graphitic anode Li_xC_6 ($0 < x \leq 1$) materials [39, 40]. It also can be seen that the expansion of the material presents different trends on each intercalation stage. At voltages higher than 200 mV (dilute stage 4), the graphite electrode expanded very rapidly. Then, the electrode expands almost linearly with a change in slope (stages 3 and 2, reaching anode lithiation degrees of x= 0.22 and x = 0.5 at the end of the stage, respectively). Finally, electrode expands significantly during stage 1 (< 0.05 V vs Li, x= 1, which corresponds to gold coloured particles as observed in Figure 4).

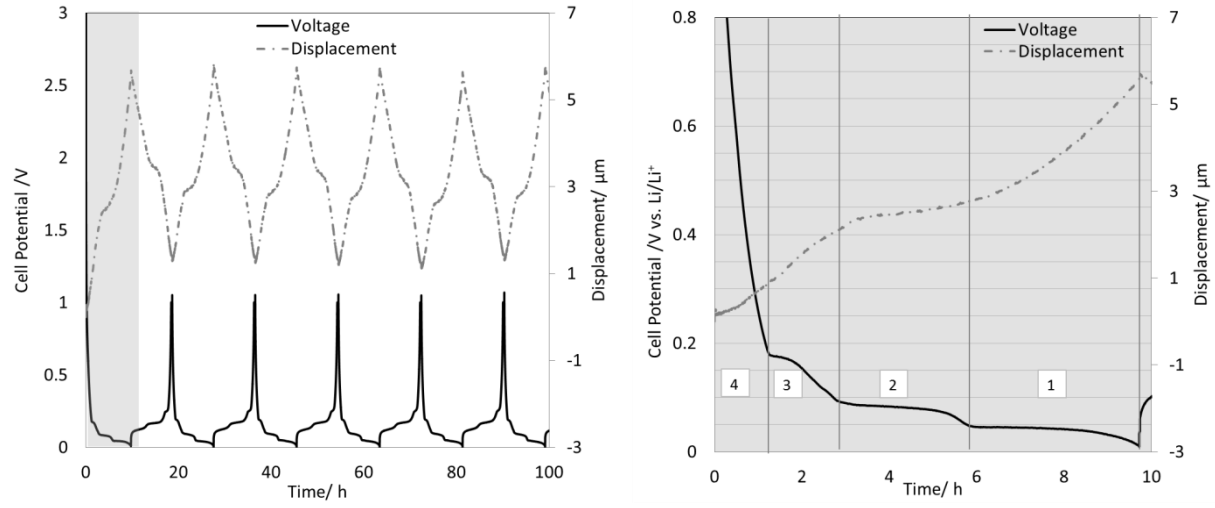

a) b)

Figure 7: a) Charge - discharge profile and electrode thickness displacement for a Gr - Li three electrode cell, b) closer look to the first intercalation step (grey area in a) where stages 4 to 1 of the intercalation can be identified

3.5 Microstructure determination

3.5.1 Scanning Electron Microscopy of battery electrodes

Scanning electron microscopy (SEM) was carried out on harvested material from a fresh A123 (1.1 Ah) cell. The opening of the 18650 cell was carried out as described in 2.2. Afterwards, samples from the extracted jelly roll were cut and washed thoroughly with dimethyl carbonate (DMC) for the removal of residual electrolyte salt ($LiPF_6$). Images for the anode (graphite) and cathode (lithium iron phosphate) are displayed in Figure 8(a, b) and (c, d), respectively. Graphite electrodes show the typical flake-like morphology of several microns in size. Additional features could be seen upon higher magnification (Figure 8b) in the form of fibres agglomerated in various cavities of the electrode. These carbon fibres might act as conductive additives in the electrode. Figure 8c shows an image of the cathode featuring a damaged electrode which possibly occurred during manipulation. At a higher magnification, 50 KX (Figure 8d), the nanoparticle structure of the material can be seen, with primary particle sizes (mostly spindle-like) around 50 nm showing agglomeration.

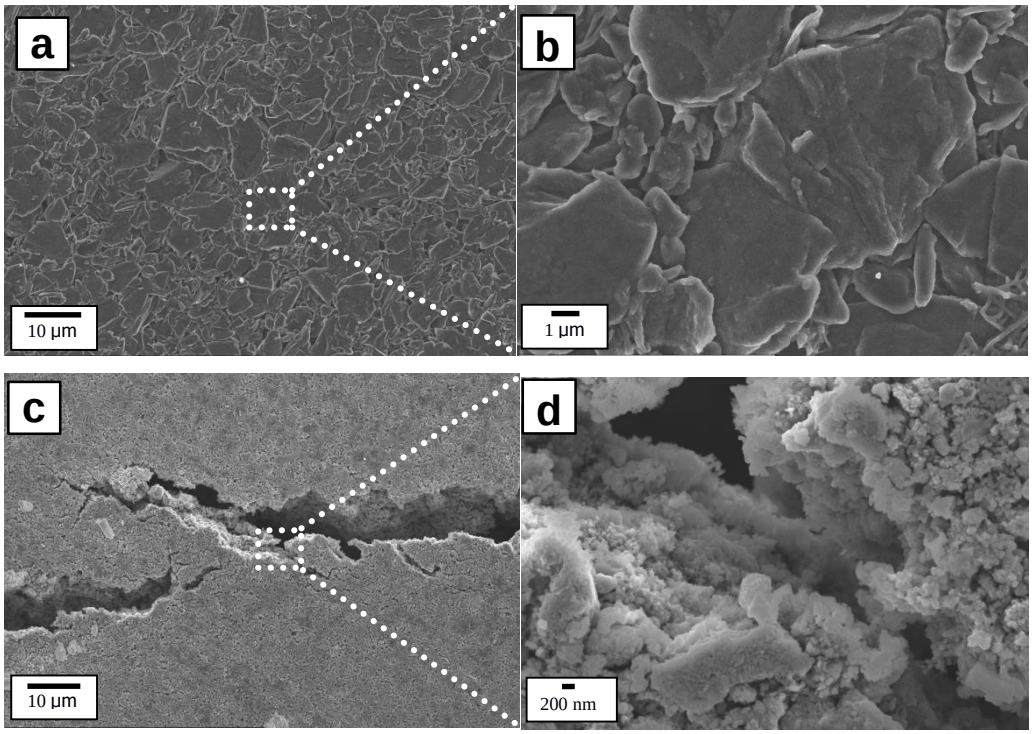

Figure 8: Scanning electron microscopy of a) and b) a graphite electrode, c) and d) a lithium iron phosphate electrode at different magnifications

3.5.2 Micro X-ray computed tomography of battery cells

Micro-X-ray computed tomography has been used for battery and supercapacitors cells [26, 41, 42]. Figure 9 shows an 18650 cell (A123-APR18650M1): on the left, a vertical cross-section is shown, where the jelly roll can be clearly recognized. Underneath the bottom end of the cell, the sample holder – a glass stick – is visible, while artefacts can be observed at the top of the cell as the rotation axis was chosen parallel to the symmetry axis of the cell. In the centre of Figure 9, three horizontal cross-sections at different heights are shown. Top and bottom cross-sections show a non-complete filling of the jelly roll with active material. A zoom-in of the central horizontal cross-section is shown at the bottom right: A layered sub-structure in the jelly roll can clearly be observed.

Finally, at the top right, a 3D reconstruction of a complete cell with a virtual cut-out to illustrate the interior of the cell is shown. Also the anode current collector is visible at the bottom of this cut-out (as also in horizontal cross-sections).

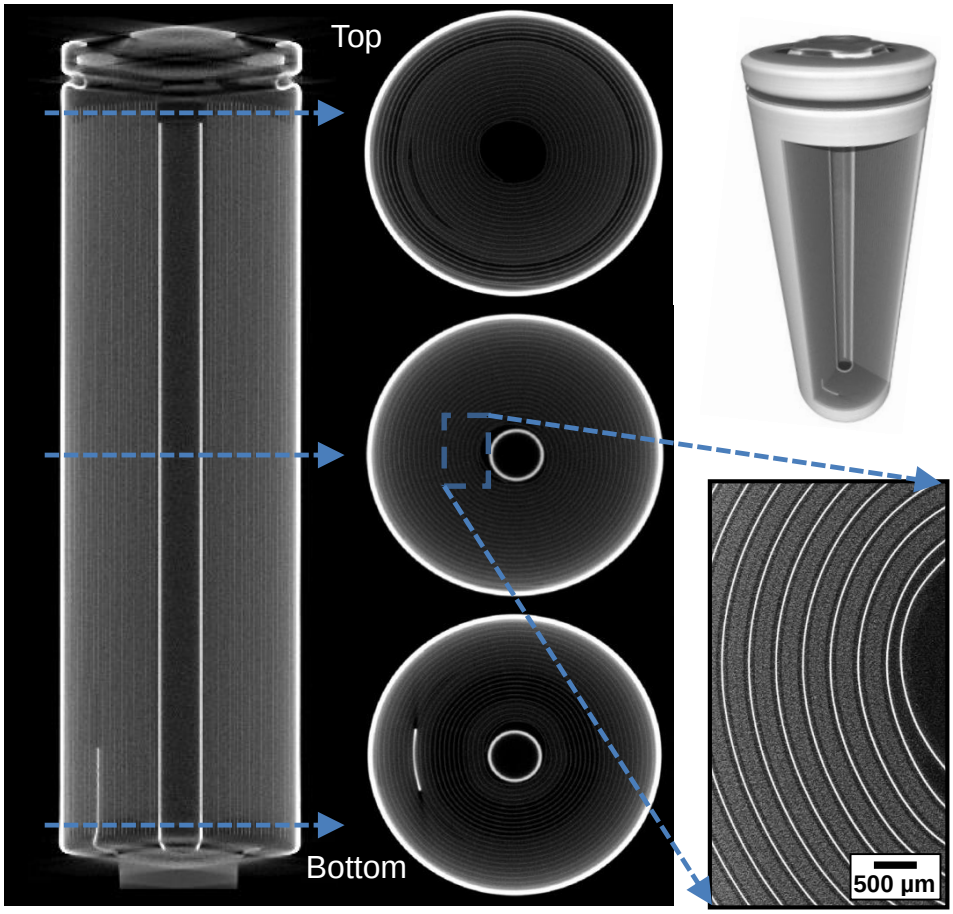

Figure 9: A123-APR18650M1 18650 cell (diameter 18 mm, height 65 mm) as investigated by micro X-ray computed tomography: a vertical cross-section is shown on the left, three horizontal cross-sections are shown in the centre (for a zoom-in see bottom right) and a 3D reconstruction of a complete cell with a virtual cut-out is shown at the top right.

X-ray computed tomography was successfully applied for the investigation of a cell and it was shown that the resolution is sufficient to gain valuable insight about microstructure. Micro X-ray CT could not only allow determination of precise microstructure, but could also serve a better understanding of degradation mechanisms (e.g. by helping identify relevant locations for material harvesting), of cell-to-cell discrepancies or in-depth analysis of samples after abuse testing.

4 Conclusions and outlook

The laboratory for battery materials and cell performance testing at JRC in Petten, Netherlands is presented and key equipment for performance assessment was shown (see 2). This laboratory can contribute on one hand towards improved understanding of degradation processes and battery technology in general and, on the other hand, towards policies which are based on robust scientific research (see e.g. 3.1).

Nevertheless, it is clear that not all questions related to safe electrification of transport can be addressed by research on material and cell level alone. For this, reason, a further extension of the JRC laboratories for battery testing is foreseen: i) a pack performance testing facility will include a walk-in environmental chamber batteries up to 100 kWh and a new dedicated X-ray computed tomography for 3-dimensional in-situ imaging of batteries up to 25 kWh under controlled environmental conditions (also during charging or

discharging); and ii) a cell safety testing facility will comprise four chambers for mechanical, electrical and thermal abuse testing of cells complemented by gas analysis.

Once the complete laboratory is operational, it will not only allow the safety assessment of cells and battery assemblies and the fitness of related testing methods and standards, but also the evaluation of potential new materials and technologies with respect to performance and safety.

Acknowledgements

The excellent support from JRC colleagues – the JRC Petten workshop especially for their work on cell opening and Marc Steen for reviewing this manuscript – is acknowledged.

References

[1] *COMMUNICATION FROM THE COMMISSION TO THE EUROPEAN PARLIAMENT, THE COUNCIL, THE EUROPEAN ECONOMIC AND SOCIAL COMMITTEE AND THE COMMITTEE OF THE REGIONS, A Roadmap for moving to a competitive low carbon economy in 2050*, COM(2011) 112, European Commission, 2011

[2] *COMMUNICATION FROM THE COMMISSION TO THE EUROPEAN PARLIAMENT, THE COUNCIL, THE EUROPEAN ECONOMIC AND SOCIAL COMMITTEE AND THE COMMITTEE OF THE REGIONS, A policy framework for climate and energy in the period from 2020 to 2030*, COM(2014) 15, European Commission, 2014

[3] *COMMUNICATION FROM THE COMMISSION, EUROPE 2020, A strategy for smart, sustainable and inclusive growth*, COM(2010) 2020, European Commission, 2010

[4] *COMMUNICATION FROM THE COMMISSION TO THE EUROPEAN PARLIAMENT AND THE COUNCIL, European Energy Security Strategy*, SWD(2014) 330, European Commission, 2014

[5] *COMMUNICATION FROM THE COMMISSION TO THE EUROPEAN PARLIAMENT, THE COUNCIL, THE EUROPEAN ECONOMIC AND SOCIAL COMMITTEE AND THE COMMITTEE OF THE REGIONS, Clean Power for Transport: A European alternative fuels strategy*, COM(2013) 17, European Commission, 2013

[6] *WHITE PAPER. Roadmap to a Single European Transport Area – Towards a competitive and resource efficient transport system*, COM(2011) 144, European Commission, 2011

[7] *REGULATION (EU) No 333/2014 OF THE EUROPEAN PARLIAMENT AND OF THE COUNCIL of 11 March 2014 amending Regulation (EC) No 443/2009 to define the modalities for reaching the 2020 target to reduce CO_2 emissions from new passenger cars*, Official Journal of the European Union, 2014

[8] *REGULATION (EC) No 443/2009 OF THE EUROPEAN PARLIAMENT AND OF THE COUNCIL of 23 April 2009 setting emission performance standards for new passenger cars as part of the Community's integrated approach to reduce CO_2 emissions from light-duty vehicles*, Official Journal of the European Union, 2009

[9] *DIRECTIVE 2014/94/EU OF THE EUROPEAN PARLIAMENT AND OF THE COUNCIL of 22 October 2014 on the deployment of alternative fuels infrastructure*, Official Journal of the European Union, L 307 (2014), 1-20

[10] *COMMUNICATION FROM THE COMMISSION TO THE EUROPEAN PARLIAMENT, THE COUNCIL, THE EUROPEAN ECONOMIC AND SOCIAL COMMITTEE AND THE COMMITTEE OF THE REGIONS, EUROPE ON THE MOVE, An agenda for a socially fair transition towards clean, competitive and connected mobility for all*, COM(2017) 283, European Commission, 2017

[11] *Declaration of Intent for Action 7 of the Integrated SET-Plan "Become competitive in the global battery sector to drive e-mobility forward"*, https://setis.ec.europa.eu/implementing-integrated-set-plan/batteries-e-mobility-and-stationary-storage-ongoing-work, accessed 30/06/2017

[12] *Letter of Intent for Cooperation between the United States Department of Energy and the Joint Research Centre of the European Commission on Electric Vehicle - Smart Grid Interoperability Centres*, 2011, www.transportation.anl.gov/pdfs/LOI.pdf, accessed 2014

[13] *Battery Energy Storage Testing for Safe Electric Transport (BESTEST)*, 2015, https://ec.europa.eu/jrc/en/research-facility/battery-energy-storage-testing-safe-electric-transport, accessed 03/08/2016

[14] *Interoperability and e-mobility*, 2014, https://ec.europa.eu/jrc/en/research-topic/interoperability-and-e-mobility, accessed 24/02/2015

[15] *Hydrogen and fuel cells* 2015, https://ec.europa.eu/jrc/en/research-topic/hydrogen-and-fuel-cells, accessed 28/07/2016

[16] *UNECE (United Nations Economic Commission for Europe) Website*, www.unece.org, accessed 29/06/2017

[17] N.P. Lebedeva, L. Boon-Brett, *Considerations on the Chemical Toxicity of Contemporary Li-Ion Battery Electrolytes and Their Components*, Journal of the Electrochemical Society, 163 (2016), A821-A830

[18] A. Pfrang, A. Kriston, V. Ruiz, N. Lebedeva, F. di Persio, *Safety of Rechargeable Energy Storage Systems with a focus on Li-ion Technology*, in: L.M. Rodriguez-Martinez, N. Omar (Eds.) *Emerging Nanotechnologies in Rechargeable Energy Storage Systems*, Elsevier, Boston, 2017, pp. 253-290

[19] *Electric Vehicle Safety (EVS)* https://www2.unece.org/wiki/pages/viewpage.action?pageId=3178628, accessed 03/08/2016

[20] V. Ruiz, A. Pfrang, A. Kriston, N. Omar, P.V.d. Bossche, L. Boon-Brett, *A Review of International Abuse Testing Standards and Regulations for Lithium Ion Batteries in Electric and Hybrid Electric Vehicles*, Renewable and Sustainable Energy Reviews, (2017), accepted for publication

[21] *Collaboration Agreement signed between JRC and EGVIA on electric vehicle battery testing*, 2015, http://www.egvi.eu/mediaroom/42/22/Collaboration-Agreement-signed-between-JRC-and-EGVIA-on-electric-vehicle-battery-testing, accessed 28/07/2016

[22] A. Kriston, A. Pfrang, V. Ruiz, I. Adanouj, T. Kosmidou, J. Ungeheuer, H. Döring, B. Fritsch, L. Boon-Brett, *External short circuit performance of NCA and NCM Li-ion cells at different external resistances*, Journal of Power Sources, (2017), accepted for publication

[23] A. Kriston, A. Pfrang, B.N. Popov, L. Boon-Brett, *Development of a full layer pore-scale model for the simulation of electro-active material used in power sources*, Journal of the Electrochemical Society, 161 (2014), E3235-E3247

[24] Z. Farkas, I. Faragó, Á. Kriston, A. Pfrang, *Improvement of accuracy of multi-scale models of Li-ion batteries by applying operator splitting techniques*, J. Comput. Appl. Math., 310 (2017), 59-79

[25] A. Pfrang, S. Didas, G. Tsotridis, *X-ray computed tomography of gas diffusion layers of PEM fuel cells: Segmentation of the microporous layer*, Journal of Power Sources, 235 (2013), 81-86

[26] A. Pfrang, *X-ray computed tomography of electrochemical power sources*, AABC (Advanced Automotive Battery Conference) Europe 2013, Strasbourg, France, 2013

[27] V. Ruiz, A. Kriston, I. Adanouj, M. Destro, D. Fontana, A. Pfrang, *Degradation Studies on Lithium Iron Phosphate - Graphite Cells. The Effect of Dissimilar Charging – Discharging Temperatures*, Electrochimica Acta, 240 (2017), 495-505

[28] M. Fleischhammer, T. Waldmann, G. Bisle, B.-I. Hogg, M. Wohlfahrt-Mehrens, *Interaction of cyclic ageing at high-rate and low temperatures and safety in lithium-ion batteries*, Journal of Power Sources, 274 (2015), 432-439

[29] R. Zhao, S. Zhang, J. Liu, J. Gu, *A review of thermal performance improving methods of lithium ion battery: Electrode modification and thermal management system*, Journal of Power Sources, 299 (2015), 557-577

[30] F. Feng, R. Lu, C. Zhu, *A combined state of charge estimation method for lithium-ion batteries used in a wide ambient temperature range*, Energies, 7 (2014), 3004-3032

[31] E.P. Roth, C.C. Crafts, D.H. Doughty, J. McBreen, *Thermal abuse performance of 18650 Li-ion cells*, Sandia National Laboratories, SAND2004-0584, 2004

[32] E.P. Roth, D.H. Doughty, *Thermal abuse performance of high-power 18650 Li-ion cells*, Journal of Power Sources, 128 (2004), 308-318

[33] IEC 62660-2: Rechargeable Cells Standards Publication Secondary lithium-ion cells for the propulsion of electric road vehicles. Part 2: Reliability and abuse testing, 2011

[34] J.R. Dahn, *Phase diagram of Li_xC_6*, Physical Review B, 44 (1991), 9170-9177

[35] S.J. Harris, A. Timmons, D.R. Baker, C. Monroe, *Direct in situ measurements of Li transport in Li-ion battery negative electrodes*, Chemical Physics Letters, 485 (2010), 265-274

[36] T. Zheng, J.N. Reimers, J.R. Dahn, *Effect of turbostratic disorder in graphitic carbon hosts on the intercalation of lithium*, Physical Review B, 51 (1995), 734-741

[37] B. Fortunato, P. Mirone, G. Fini, *Infrared and Raman spectra and vibrational assignment of ethylene carbonate*, Spectrochimica Acta Part A: Molecular Spectroscopy, 27 (1971), 1917-1927

[38] J.O. Besenhard, M. Winter, J. Yang, W. Biberacher, *Filming mechanism of lithium-carbon anodes in organic and inorganic electrolytes*, Journal of Power Sources, 54 (1995), 228-231

[39] M. Bauer, M. Wachtler, H. Stöwe, J.V. Persson, M.A. Danzer, *Understanding the dilation and dilation relaxation behavior of graphite-based lithium-ion cells*, Journal of Power Sources, 317 (2016), 93-102

[40] T. Ohzuku, Y. Iwakoshi, K. Sawai, *Formation of lithium graphite intercalation compounds in nonaqueous electrolytes and their application as a negative electrode for a lithium ion (shuttlecock) cell*, Journal of the Electrochemical Society, 140 (1993), 2490-2498

[41] D.P. Finegan, M. Scheel, J.B. Robinson, B. Tjaden, I. Hunt, T.J. Mason, J. Millichamp, M. Di Michiel, G.J. Offer, G. Hinds, D.J.L. Brett, P.R. Shearing, *In-operando high-speed tomography of lithium-ion batteries during thermal runaway*, Nature Communications, 6 (2015),

[42] J. Gonzalez, K. Sun, M. Huang, J. Lambros, S. Dillon, I. Chasiotis, *Three dimensional studies of particle failure in silicon based composite electrodes for lithium ion batteries*, Journal of Power Sources, 269 (2014), 334-343

Authors

After graduating from the University of Texas at Austin, **Andreas Pfrang** received his PhD in physics at the University of Karlsruhe, Germany, in 2004. After providing microscopy services as team leader at Freudenberg Forschungsdienste in Weinheim, Germany, in 2007 he joined the European Commission's Joint Research Centre in Petten, Netherlands. There he performed fuel cell related research and was responsible for the microscopy services of the Institute for Energy and Transport until end of 2012. Since January 2013 he has contributed to a new project on battery energy storage testing for safe electrification of transport (BESTEST) at the Joint Research Centre.

Franco Di Persio obtained his PhD in material engineering from the Swansea University, Swansea (UK) in 2004. After some years in the private sector he joined the European Commission's Joint Research Centre (JRC) in 2014. He is currently a Scientific / Technical Support Officer at the electric vehicle battery testing group at the JRC –Directorate for Energy, Transport & Climate.

Akos Kriston obtained his PhD in 2012 in electrochemistry from Eotvos Lorand Science University, (Hungary). During his PhD he developed 3 award winning fuel cell and battery vehicles. After graduation he worked as a post-doc fellow at the University of South Carolina for 1 year. Since 2013 he works for the European Commission's Joint Research Centre in Petten as part of the battery energy storage testing for safe electrification of transport (BESTEST) project.

Natalia Lebedeva obtained her PhD in physical chemistry and electrocatalysis from Eindhoven University of Technology (The Netherlands) in 2002. From 2002 to 2011 she was a (senior) scientist at the Energy Research Centre of the Netherlands (ECN) leading projects on development of proton-exchange fuel cells for automotive applications. From 2011 to 2013 she worked as a project manager at the Maritime Materials Performance Centre of TNO, leading research on corrosion and corrosion protection in extreme environments. In 2013 she joined the battery energy storage testing for safe electrification of transport (BESTEST) team at the European Commission's Joint Research Centre in Petten.

Vanesa Ruiz obtained her PhD in materials science at the University of Oviedo in 2008. Then she obtained a postdoctoral fellowship at the Energy Technology Division (Energy storage/supercapacitors group), CSIRO, Australia and a Juan de la Cierva fellowship at the Research Centre for Nanoscience and Nanotechnology (CIN2) of the Spanish National Research Council (CSIC). Expert in the synthesis of active electrode materials for supercapacitors (activated carbons, graphene-based materials, nanoparticles doping, electrodeposition of metal oxides, etc.), electrochemical characterization and testing. Presently working as Scientific Officer, at the European Commission's Joint Research Centre in the Netherlands dealing with battery testing for safe electrification of transport.

Denis Dams graduated from the secondary technical school, electro-mechanical department, in Geel, Belgium. Since April 1986, he is employed at the European Commission's Joint Research Centre in Petten, The Netherlands, where he worked in the experimental department of the high flux reactor (HFR) until 1999. Since December 1999 he has been responsible for the Process Simulation Test Laboratory (PSTL) as lab manager, where now battery testing is performed. He contributed to these new experimental activities by evaluating requirements concerning safety, environment, translating these requirements into technical solutions and integrating the new test setups into the existing PSTL infrastructure.

Theodora Kosmidou graduated from the Physics Department and received her MSc and PhD in Polymer Science and Technology from the University of Patras, Greece. She has worked in the field of physics and materials science in universities in Greece from 1999 till 2008. In 2009 she joined the European Commission's Joint Research Centre in Petten, Netherlands, where she initially worked with structural materials for nuclear applications. Since 2013 she is a member of the project team on battery energy storage testing for safe electrification of transport (BESTEST) at the Joint Research Centre.

After the graduation in technical physics on the TH Aachen, **Jürgen Ungeheuer** worked on solar systems, a linear accelerator and cooler synchrotron (COSY) in the Forschungszentrum Jülich, Germany. After moving to the Joint Research Centre Petten in 1987, he was involved in material research for high temperature applications (silicon carbide, silicon nitride) and in biomass conversion (fluidized bed gasification). In 2013 he joined the team for a new project on Battery Energy Storage Testing for Safe Electrification of Transport (BESTEST) at the Joint Research Centre.

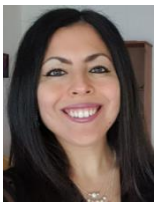

After having a BSc in chemistry and a specialization in biotechnology from Institut Paul Lambin, Université Catholique de Louvain (Belgium), **Ibtissam Adanouj** has worked more than 6 years at ExxonMobil Chemical Europe contributing with her analytical chemistry skills to different R&D projects and to some process optimization conducted on pilot plants. In December 2010, she joined the European Commission's Joint Research Centre in Petten, Netherlands where she was responsible for developing analytical methods for biomass characterization. Since April 2016, she works as part of the battery energy storage testing for safe electrification of transport (BESTEST) project.

Lois Brett obtained her PhD in Combustion Chemistry from the National University of Ireland, Galway in 1999. She initially joined the European Commission's Joint Research Centre in Petten, The Netherlands in 2002 in a postdoctoral role testing high pressure hydrogen storage systems and hydrogen safety sensors. Following this she worked at the Rocket Technology Group of TNO in The Netherlands for over 2 years developing a solid gas generator technology for hydrogen storage. She re-joined the European Commission in 2007 to continue the work on hydrogen safety sensor performance testing and application. Since 2013 she leads the battery energy storage testing for safe electrification of transport (BESTEST) activity.